Lowland Technology International 2015; 17 (2): 59-72
International Association of Lowland Technology (IALT): ISSN 1344-9656

Research Paper

Evaluation of settlement behavior of the improved ground by using floating type columns during consolidation

Z.B. Jiang [1], R. Ishikura [2] and N. Yasufuku [3]

ARTICLE INFORMATION

Article history:

Received: 13 April, 2015
Received in revised form: 03 June, 2015
Accepted: 16 June, 2015
Publish on: September, 2015

Keywords:

Floating type cement-treated columns
Time-dependent skin friction
Consolidation
Settlement

ABSTRACT

For soft soil engineering, in many cases, the foundation directly on natural ground cannot satisfy the requirement, such as embankment on deep soft clay layer. Consequently, a technology of combining the float-type cement-treated columns and surface stabilization is developed for reducing the settlement and the construction cost. In order to apply this technology for practice, it is important to predict the total settlement of the ground in relation to the important factors. In this paper, in order to evaluate the consolidation settlement behavior, a time-dependent skin friction model for the column-soil interaction is developed to describe the nonlinear relationship between column shaft shear stresses and effective vertical pressure in the surrounding soft clay. The time-dependent equivalent skin friction length which treating a part of floating type improved ground with a length of αH_1 as an unimproved portion can be obtained based on a homogenization theoretical method. The compression settlement of this unimproved portion can be computed using the properties of soft clay alone. For verifying the effectiveness of this method, a set of laboratory model tests were performed. Furthermore, the settlement behavior and stress distribution characteristics were investigated by image analysis.

1. Introduction

In the past several decades, there has been an increasing recognition that the composite technology has significant contribution to the ground improvement construction. Composite method, such as those proposed by Balaam et al. (1977), Priebe (1995), Bergado et al. (1994), Poungchompu et al. (2010), Zhang et al. (2012), Maheshwari and Khatri (2012) and Ng and Tan (2014a) are commonly used to calculate the settlement of soft ground improved by column type inclusions.

However, for deep soft soil layer, to reduce the construction cost and minimize the impact on the ground environment, a technology combined with ground improvement methods such as float-type cement-treated columns, surface stabilization, and lightweight embankment methods has been developed, which is perceived as one of the effective and acceptable methods for improving the soft clay ground.

[1] Ph.D. Candidate, Department of Civil Engineering, Kyushu University, Fukuoka 819-0395, JAPAN, jzb926@163.com
[2] Assistant Professor & IALT member, Department of Civil Engineering, Kyushu University, Fukuoka, 819-0395, JAPAN, ishikura@civil.kyushu-u.ac.jp
[3] Professor & IALT member, Department of Civil Engineering, Kyushu University, Fukuoka, 819-0395, JAPAN, yasufuku@civil.kyushu-u.ac.jp
Note: Discussion on this paper is open until December 2015

Figure 1 shows the concept of floating type ground improvement. As shown in Fig. 1, this type of technique can be useful for deep soft soil layer considering that it can reduce the settlement. Consequently, in order to apply this technology for practice, several important aspects need to be discussed in advance. For this structural form, it is important to predict the total settlement of the ground in relation to the important factors. During consolidation, the skin friction between the columns and soft clay will occur (Randolph, 1983; Poulos, 1994; Jamsawang, 2009), which plays an important role in reducing ground settlement.

In previous studies, several investigations for considering the influence of the improvement parameters have already been conducted by Lee (1993), Randolph et al. (1979), Miki and Nozu (2004), Pribe (1995), Ishikura et al. (2007, 2013) and Ng and Tan (2014b). A method for predicting the total settlement of this improvement ground has already been proposed by Ishikura et al. (2008, 2009).

In this paper, in order to evaluate consolidation settlement in consideration to skin friction characteristics, a time-dependent skin friction model for the column-soil interaction is developed. In order to clarify the practicability of this model, a set of model tests in three different test conditions which is improved by using different number of model columns were performed under one-dimensional plane strain condition, respectively. Settlement behavior and strain distribution characteristics were investigated by image analysis. By comparing the test and calculated results, the influence of the skin friction and ground improvement ratio a_p during the consolidation settlement were investigated. (a_p means the ratio between the sum of cross-sectional area of all columns and total cross-sectional area of the improved ground).

2. Methodology for predicting time-dependent consolidation settlement

In this section, a method based on homogenized theory with a consideration of the stress distribution ratio a_p is proposed. As mentioned above, the floating type column improved layer is composed of two types of compression portion. The compression of unimproved portion can be calculated by the properties of the soft soil alone, whose characteristics are treated as same as the subsoil layer (H_2 in Fig. 1). The key point of the proposed method is to determine the length of time-dependent unimproved portion.

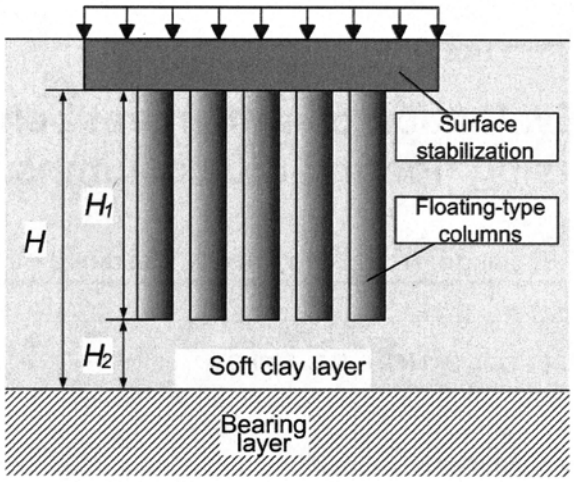

Fig. 1. Schematic diagram of improved ground by floating-type columns.

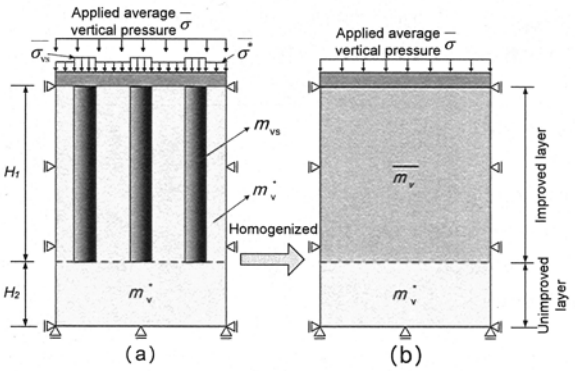

Fig. 2. Schematic diagram of the homogenized composite ground.

2.1 *Principles of homogenization method*

The main components of this improved ground are soft soil and improved columns. Aiming to obtain the compression of mixed ground, the improved portion is assumed as a homogeneous mass, which can be presented by the homogenized material parameters (Omine and Ochiai 1992; Omine et al., 1998), as shown in Fig. 2(b). In vertical direction, the average coefficient of volume compressibility of composite portion can be calculated as following:

$$\overline{m_v} = \frac{a_p \bar{n} m_{vs} + (1 - a_p) m_v^*}{(\bar{n} - 1) a_p + 1} \quad [1]$$

where m_{vs} and m_v^* are the coefficient of volume compressibility of columns and surrounding soil, respectively, and $\bar{n}$ is stress distribution ratio, defined as the vertical stress applied on improved column and surrounding soft soil within a unit cell consisting of a column and soil (Chai and Carter, 2011), as shown in Fig. 2(a):

$$\bar{n} = \frac{\overline{\sigma_{vs}}}{\overline{\sigma^*}} \quad [2]$$

where $\overline{\sigma_{vs}}$ and $\overline{\sigma^*}$ are the average stress in column and surrounding soil, respectively.

After the overburden being applied, there will be penetration of the columns into the underlying soft clay layer. According to the currently design methods (JICE) and the results of model tests and FEM analysis, (Figs. 15 and 17 in sections 3 and 4, respectively), the improved layer (H_1) is classified as two portions. Ishikura et al. (2007, 2008, 2009) proposed a method to calculate the thickness of unimproved portion based on homogenization theory. As mentioned in his method, one of the most important factors is the unimproved layer thickness ratio α, which is defined as the ratio of the divided unimproved layer thickness to the whole improved length H_1 (Fig. 3), The formula of α can be expressed as following:

$$\alpha = \frac{\overline{m_v} - \overline{m_{vf}}}{\overline{m_v^*} - \overline{m_{vf}}} \quad [3]$$

where $\overline{m_{vf}}$ denotes the average coefficient of volume compressibility of the confining portion which is defined as the equivalent foundation (Fig. 3(b)). The value of $\overline{m_{vf}}$ can be obtained by substituting the rigidity ratio between columns and soft soil $n_f = \overline{n} = m_v^*/m_{vs}$ in Eq. [1]. Moreover, the value of α will be changed during consolidation process.

For estimating the average coefficient of volume compressibility of the composite ground $\overline{m_v}$, the stress distribution ratio $\overline{n}$ should be confirmed. As exhibited in Fig. 4(a), the columns and soft clay are assumed as independent compressional mass with different rigidity and upward skin friction generated. These compressional mass deform independently in proportion to the stress applied on them. The composite ground is mainly composed of two kinds of element body, element Ⅰ and element Π illustrated in Fig. 4(b). Since the composite foundation was taken as a whole, the same settlements of these two elements are produced, i.e. SⅠ = SΠ, hence, the stress distribution ratio $\overline{n}$ can be rewritten as Eq. [4],

$$\bar{n} = \frac{(H_1/H_2+1)\bar{\sigma} + \bar{\tau}A_c/(2A_0a_p)}{\left[H_1m_{vs}/(H_2m_v^*)+1\right]\bar{\sigma} - \bar{\tau}A_c/\left[2A_0(1-a_p)\right]} \quad [4]$$

where $\overline{\tau}$ is the unit skin friction applied on column shaft, A_c is the total cross-sectional area of the columns, and A_0 is the total cross-sectional area of the improved ground. It is shown that the unimproved layer thickness ratio α is a function of skin friction $\overline{\tau}$, which can be computed by combining Eqs. [1], [3] and [4] when $\overline{\tau}$ is available.

2.2 Time-dependent skin friction

The most important factor for evaluating the stress distribution ratio in Eq. [4] is to formulate the skin friction. For this kind of improved ground, loading on ground surface will cause compression and consolidation settlement. Column-soil relative displacement increases subsequently, and action exerting on interface skin friction is reinforced, resulting in augment onto the interface skin friction. The combined foundation transfers the load to the column group via the surface stabilization, hence soft clay between the friction columns in the upper part of the combined foundation is enclosed. The ground surface was deformed equally by the rigid stabilization on the assumption of shallow stabilized ground.

2.3 Time-dependent skin friction

In order to calculate the skin friction considering ground consolidation, a hypothesis of skin friction around the surface of columns on account of column-soil relative displacement is presented as displayed in Fig. 5. The

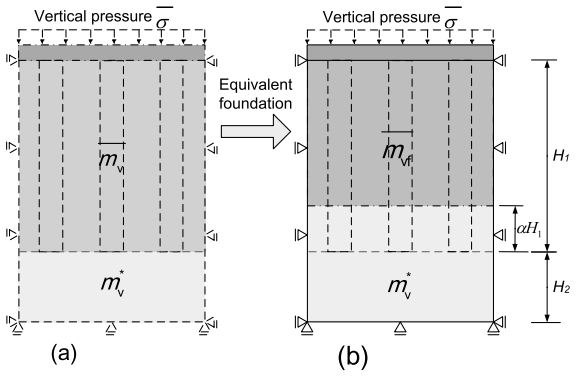

Fig. 3. Schematic diagram showing of unimproved layer thickness ratio α.

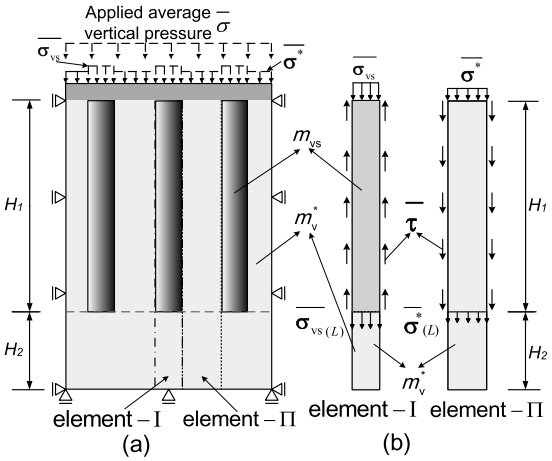

Fig. 4. Schematic diagram of the homogenized composited ground.

relative displacement curve is obtained based on image analysis of laboratory model test results in section 3 and FEM analysis results in section 4. During ground consolidation process, the length of column-soil relative displacement changed over time, moreover, the total skin friction aroused by relative displacement can be equivalent to a total skin friction within an equivalent skin friction length, shown as in Fig. 5(b), area I = area Π. The column-soil skin friction used for supporting upper load is totally derived from equivalent skin friction. The whole upper load can transfer to the soft soil of unimproved layer. As a result, the equivalent skin friction length can be represented by the time-dependent unimproved layer thickness, $\alpha(t)H_1$, which is exhibited in Fig. 6.

Generally, the column soil interface resistance is expressed as Eq. [5].

$$\tau = K\sigma_v' \tan\delta' \quad [5]$$

where, τ is the interface skin friction, K is the lateral earth pressure coefficient, σ'_v is the effective overburden pressure, and δ' is the effective friction angle of column-soil interface. The angle δ' depends on the nature of the column shaft and surrounding soil, and can be reasonably determined using shear box tests or ring shear tests. For practical purposes, it is often assumed to be equal to a fraction of the angle of the shearing resistance of the surrounding soil, ϕ'. The coefficient K depends on various factors including the state of the soil, the method of column installation, and the geometry of the column, it can be related to the in situ earth pressure coefficient K_0, whose value is approximately estimated by K_0 = 1-sinϕ'. Hence, Eq. [5] can be rewritten in another:

$$\tau = K_0(\frac{K}{K_0})\sigma_v' R\tan\phi' \quad [6]$$

$$R = \tan\delta'/\tan\phi' \quad [7]$$

R is the interface roughness coefficient. When R =1, it means the slip surface is in the soil mass, δ' = ϕ'; and when R < 1, i.e. δ' < ϕ', it means soil roughness is large than column shaft roughness, the slip surface will generate on the column soil interface. The relationship between shin friction and roughness coefficient can be investigated detailed using ring shear tests. Some proposals have been made for the ratios K/K_0. For example, it has been suggested that K/K_0 is in the range 0.7-1.2 for small-displacement piles and 1.0-2.0 for large-displacement piles (Kulhawy, 1984). The mainly suggested values of K are summarized in Table 1 (Zhang et al., 2012):

Owing to the special construction technique of deep mixing of cement with soft clay and water, the installation process is often carried out by employing rotary equipment with double drills or four drills, and forming a wall shape column groups. The cross section of this composited ground, therefore, can be assumed as a plane strain condition, which is also applied in model test and FEM analysis. Consequently, one-dimensional consolidation theory can be adopted for normal consolidated saturated soft clay in this technique. After applying overburden load, the effective stress in soft clay increased with time due to the excess pore water

Table 1. Suggested values of K.

Suggested values of K	Pile-soil condition	Reference
K/K_0=0.7-1.2	Smooth steel pipe piles, H-piles or concrete piles (Small-displacement piles)	Kulhawy (1984)
K/K_0=1.0-2.0	Smooth steel pipe piles, H-piles or concrete piles (Large displacement piles)	Kulhawy (1984)
K/K_0=1.0	Driven or jacked open-ended steel pile piles, Normally consolidated soil	Miller and Lutenegger (1997)
K/K_0=1.0-4.0	Driven or jacked open-ended steel pile piles, Overconsolidated clay	Miller and Lutenegger (1997)
K/K_0=1.2-1.5	Driven steel pile, Alluvium and completely decomposed granite	Yang et al. (2006)

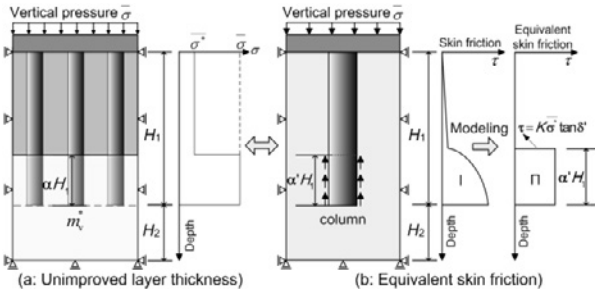

Fig. 5. Hypothesis of skin friction around the surface of columns.

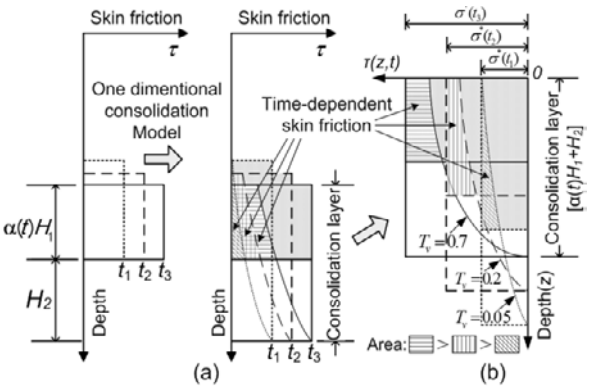

Fig. 6. Illustration of time-dependent skin friction model.

pressure dissipation. The skin friction at arbitrary time (t) and depth (z), can be calculated by Eq. [8].

$$\tau(z,t) = K_0(\frac{K}{K_0})\sigma'(z,t)R\tan\phi'' \quad [8]$$

$$\sigma'(z,t)=\sigma^*(t)-u(z,t) \quad [9]$$

where σ'(z,t) and u(z,t) are the vertical effective pressure applied on the soft soil and the excess pore pressure in the soil at random time (t) and depth (z), respectively, and $\sigma^*(t)$ is the total vertical pressure applied on the soft soil, the value of which is equal to the initial excess pore pressure $u_0(t)$ at time (t). The variation range of depth is between zero and $\alpha(t)H_1$, i.e. the length of the shaded part in Fig. 6(a). The vertical effective pressure increased during consolidating process, which caused the increment of skin friction. As illustrated in Fig. 6(b), the area covered with different lines denotes the time-dependent skin friction, it increases with time. In Fig. 6, there are three independent variables as a whole, $\sigma^*(t)$, α(t) and u(z,t), all changed by consolidating time (t). Based on Eq. [8], the summation of skin friction along the column shaft length caused by soft soil consolidation will be computed as below:

$$f(t) = K_0(\frac{K}{K_0})R\tan\phi'\int_0^{\alpha(t)H_1}\sigma'(z,t)dz \quad [10]$$

$$\int_0^{\alpha(t)H_1}\sigma'(z,t)dz = \sigma^*(t)\alpha(t)H_1 - u_0(t)\int_0^{\alpha(t)H_1}\Omega(z,t)dz \quad [11]$$

$$\Omega(z,t) = \sum_{n=0}^{\infty}\frac{2}{M}\sin\frac{Mz}{H(t)}\exp(-M^2T_v) \quad [12]$$

where, $M = (2n+1)\pi/2$, $n = 0,1,2\cdots$, $T_v = C_vt/H(t)^2$, $H(t) = \alpha(t)H_1+H_2$, t is consolidating time and H(t) is the length of the drainage path. Hence the unit skin friction can be calculated in Eq. [13].

$$\bar{\tau}(t) = f(t)/\alpha(t)H_1 \quad [13]$$

2.4 Time-dependent homogenized parameters

In accordance with time-dependent unimproved layer thickness, the homogenized parameters changed over time as well. As illustrated in Fig. 6, initially, the excess pore pressure equals to the total vertical pressure on the surrounding soil, afterwards it decreases gradually with time until reached zero. The variation range of the depth of consolidating soft soil layer is between zero and $\alpha(t)H_1+H_2$. Therefore, the total effective average vertical pressure applied on the columns and surrounding soil is represented as $\bar{\sigma}'(t)$, the value of which considering excess pore pressure can be computed as (Fig. 6b):

$$\bar{\sigma}'(t) = \bar{\sigma} - \int_0^{\alpha(t)H_1+H_2}u(z,t)dz/(\alpha(t)H_1+H_2) \quad [14]$$

$$\int_0^{\alpha(t)H_1+H_2}u(z,t)dz = u_0(t)\int_0^{\alpha(t)H_1+H_2}\Omega(z,t)dz \quad [15]$$

Here $\bar{\sigma}$ denotes the total average vertical pressure when consolidation finished. As the stress distribution ratio also will change over time, the Eq. [4], hence can be rewritten as following:

$$\bar{n}(t) = \frac{(\frac{H_1}{H_2}+1)\bar{\sigma}'(t)+\frac{\bar{\tau}(t)A_c}{2A_0a_p}}{\left(\frac{H_1m_{vs}}{H_2m_v^*}+1\right)\bar{\sigma}'(t)-\frac{\bar{\tau}(t)A_c}{2A_0(1-a_p)}} \quad [16]$$

where $\bar{n}(t)$ and $\bar{\tau}(t)$ are time-dependent effective stress distribution ratio and unit skin friction, respectively. In Eq. (16), only the effective average vertical pressure was considered. The coefficient of volume compressibility of the composite ground at a time t can be expressed as below (the coefficient of volume compressibility of columns and surrounding soil m_{vs} and m_v^* are assumed as invariants).

$$\bar{m}_v(t) = \frac{a_p\bar{n}(t)m_{vs}+(1-a_p)m_v^*}{\left[\bar{n}(t)-1\right]a_p+1} \quad [17]$$

Consequently, the time-dependent coefficient of the unimproved layer thickness ratio α(t) can be presented as:

$$\alpha(t) = \frac{\bar{m}_v(t)-\bar{m}_{vf}}{m_v^*-\bar{m}_{vf}} \quad [18]$$

2.5 Calculation of α(t)

According to Eqs. [13], [16], [17] and [18], in order to get the results of α(t), the total vertical pressure applied on the soft soil $\sigma^*(t)$ (in Eq. [10]) and the initial excess pore pressure $u_0(t)$ (in Eqs. [11] and [15]) should be confirmed firstly, however they are equal in value. Based on the definition of stress distribution ratio (Eq. [2]), the effective vertical pressure applied on the soft soil can be expressed as below:

$$\sigma'(t) = \frac{1}{\left[\bar{n}(t)-1\right]a_p+1}\bar{\sigma}'(t) \quad [19]$$

Based on field measurement, the vertical pressure applied on columns is almost invariable after construction finished, the variation of stress distribution ratio is mainly caused by the dissipation of excess pore water pressure in soft clay, i.e. $\sigma^*(t_1) = \sigma^*(t_2) = \sigma^*(t_3)$ as shown in Fig. 6(b). Therefore, it can be assumed that the total vertical pressure applied on the soft soil $\sigma^*(t)$ is a constant value,

σ^*, it resulted in the value of $u_0(t) = \sigma^*(t)$ will not change over time. The total vertical pressure applied on soil can be gained when t is positive infinity, i.e. the time when consolidation process finished, $\sigma'(t=\infty) = \sigma^*(t) = u_0(t)$. The unit skin friction at the end of construction can be calculated based on Eqs. [13] and [19], as following:

$$\bar{\tau}(t=\infty) = K_0\left(\frac{K}{K_0}\right)\tan\left[\phi'\left(\frac{\delta'}{\phi'}\right)\right]\frac{\bar{\sigma}'(t=\infty)}{\left[\bar{n}(t=\infty)-1\right]a_p+1} \quad [20]$$

where $\bar{\sigma}'(t=\infty) = \bar{\sigma}$ according to Eq. [14]. Meanwhile, the Eq. [16] should be rewritten in Eq. [21] when t is positive infinity:

$$\bar{n}(t=\infty) = \frac{\left(\frac{H_1}{H_2}+1\right)\bar{\sigma}'(t=\infty)+\frac{\bar{\tau}(t=\infty)A_c}{2A_0a_p}}{\left(\frac{H_1m_{vs}}{H_2m_v^*}+1\right)\bar{\sigma}'(t=\infty)-\frac{\bar{\tau}(t=\infty)A_c}{2A_0(1-a_p)}} \quad [21]$$

Substituting Eq. [19] into Eq . [20], the effective stress distribution ratio and unit skin friction can be obtained sequentially and in consequence according to Eq. [18], when the effective stress distribution ratio is available, $\sigma'(t=\infty) = \sigma^*(t) = \sigma^* = u_0(t) = u_0$ can be finally gained. As a consequence, in Eqs. [13] and [16], obviously, the only unknown parameter is the unimproved layer thickness ratio α(t) when time is determined. Combining Eqs. [13], [16], [17] and [18], the value if α(t) can be simultaneously solved using iterative approach.

2.6 Parametric studies

For predicting consolidation settlement of this composited ground using the proposed method, the unimproved layer thickness ratio α is one of the most important factors. It is necessary that the characteristics of α are clarified by examining the effects of various parameters on α. Figure 7 shows the relationship between unimproved layer thickness ratio α_0 and length improvement ratio H_1/H. α_0 denotes the unimproved layer thickness ratio without consideration the column-soil skin friction. The analysis is under the condition that the column radius is 0.031 m and m_v^*/m_{vs} = 136. Figure 7 shows that α_0 decreases with an increase in the improvement parameters such as improvement ratio and improvement depth. From Fig. 8 and Fig. 9, it is mainly recognized that the unimproved layer thickness ratio decreases with an increase of K/K_0 and R at the same improvement ratio condition. Moreover, for low improvement ratio, the effects are particularly evident. Meanwhile, it is noteworthy that the effect of R. The results indicate that the unimproved layer thickness ratio

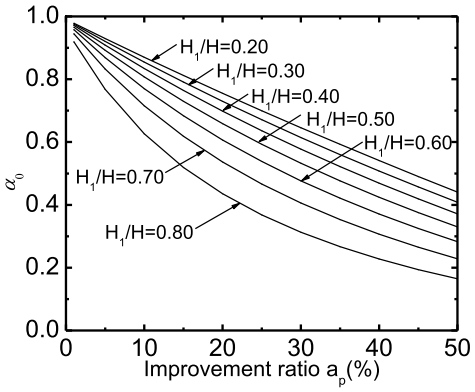

Fig. 7. Influence of improvement parameters.

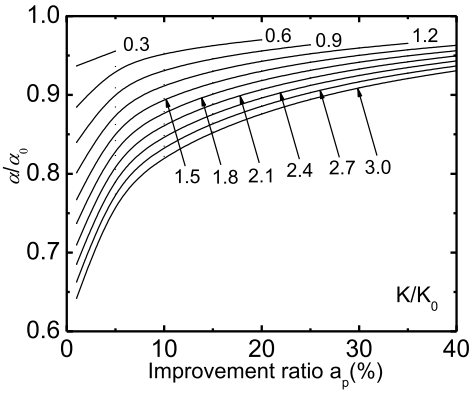

Fig. 8. Influence of soil and interface characteristics.

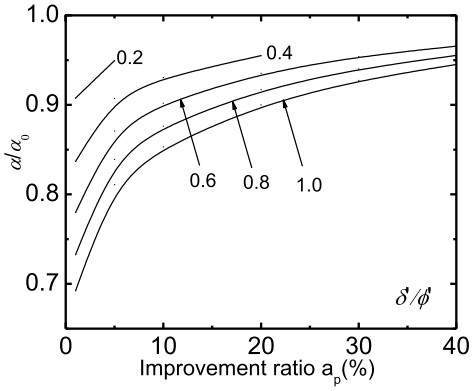

Fig. 9. Influence of soil and interface characteristics.

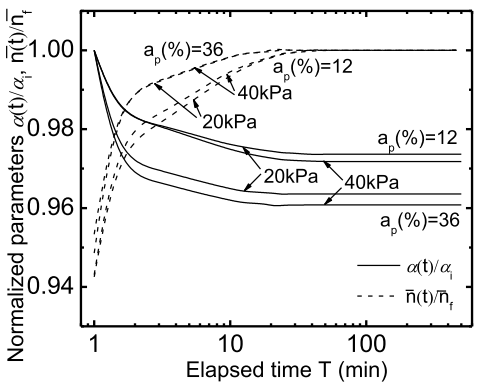

Fig. 10. Influence of soil and interface characteristics.

will decrease in case of the column surface roughness increases.

Figure 10 shows the effect of time on parameters. In this figure, α_i and $\overline{n_f}$ mean the initial unimproved layer thickness ratio and final effective stress distribution ratio under each test condition, respectively. It is obviously that the unimproved layer thickness ratio decreases with time while the effective stress distribution ratio increases with time. From this figure, however, the higher the improvement ratio, the faster the rate of variation of normalized parameters in both conditions, namely the rate of primary consolidation increased with the increase of improvement ratio.

2.7 *Settlement calculation of the composited ground*

Figure 11 shows the concept for predicting the total consolidation settlement of this improved ground. In this proposed model, the total settlement is calculated based on the summation of one-dimensional consolidation settlement of two layers, which comprising the equivalent foundation and unimproved layer. Several thicknesses of layers are determined using the time-dependent unimproved layer thickness ratio α(t) in relation to the improvement parameters, such as the improvement area and improvement length.

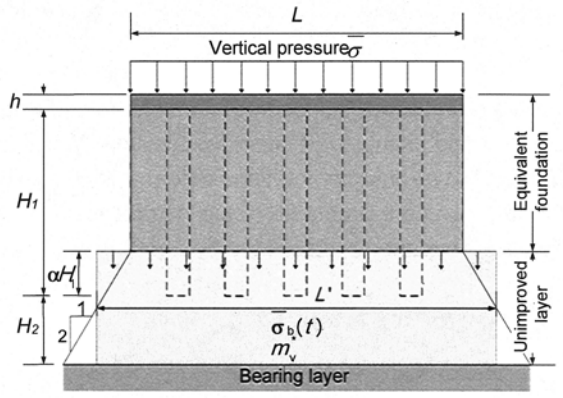

Fig. 11. Concept for calculating the total settlement of the composite ground.

The average distributive effective vertical pressure on the unimproved layer $\overline{\sigma_b}'(t)$, can be obtain by considering the effective overburden pressure $\overline{\sigma}'(t)$ at a time t based on the 2:1 method as illustrated in Fig. 11 (Bergado et al., 1994):

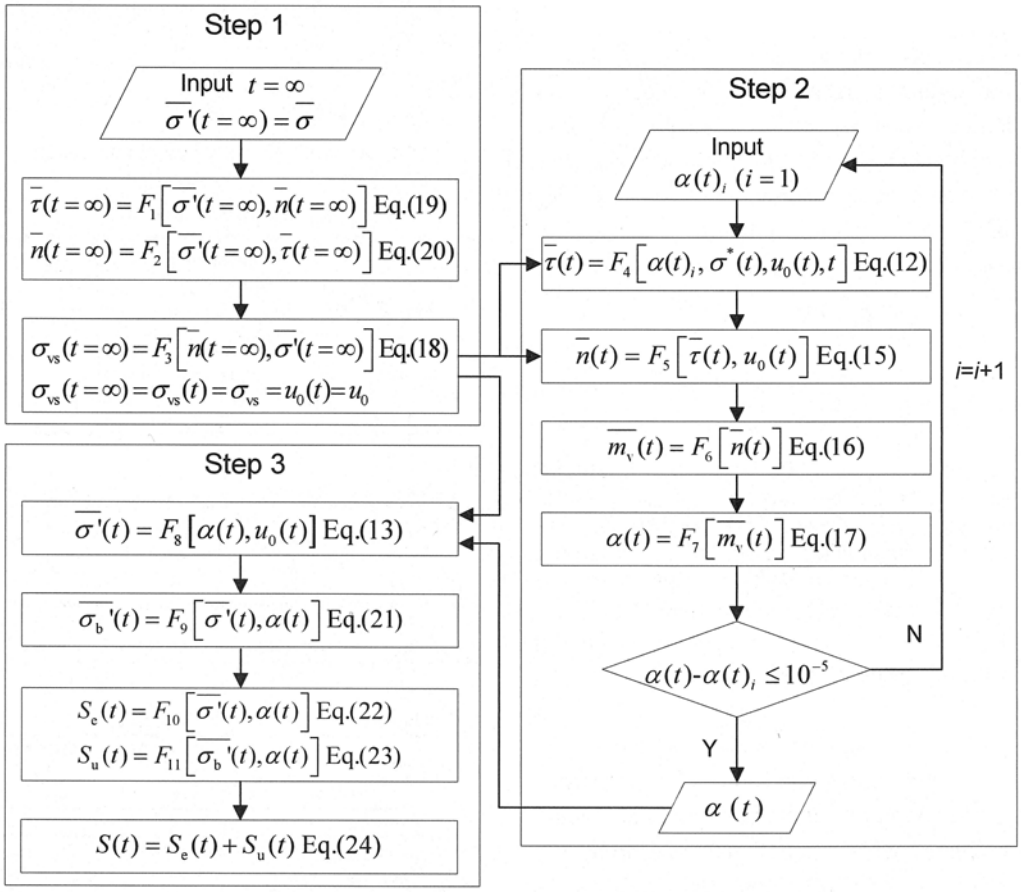

Fig. 12. Calculation flow chart of proposed method.

$$\overline{\sigma_b}'(t) = \overline{\sigma}'(t)\frac{L}{L'} = \overline{\sigma}'(t)\frac{L}{L+\left[H-(1-\alpha(t)\ )H_1\right]/2} \quad [22]$$

where L and L' are the loading width on the equivalent foundation and unimproved layer, respectively. When the unimproved layer thickness ratio is determined in relation to the improvement parameters, the compression of the equivalent foundation is calculated by Eq. (23):

$$S_e(t) = m_{vc}h\overline{\sigma} + \overline{m_{vf}}\left[1-\alpha(t)\right]H_1\overline{\sigma}'(t) \quad [23]$$

where m_{vc} and m_{vf} denote the coefficient of volume compressibility of the surface stabilization and equivalent foundation, respectively, h and H_1 are the thickness of surface stabilization and the depth of the improved layer, respectively. On the other hand, the settlement of the unimproved layer is computed as following:

$$S_u(t) = m_{vs}\left\{H-\left[1-\alpha(t)\right]H_1\right\}\overline{\sigma_b}'(t) \quad [24]$$

Ultimately, the total settlement of the improved ground at a time t can be predicted by the summation of $S_e(t)$ and $S_u(t)$, shown in following equation:

$$S(t) = S_e(t) + S_u(t) \quad [25]$$

The whole calculation process is shown in Fig. 12. $F_{1\sim11}$ denote the different equations. The procedure is mainly constituted by three parts: obtaining of total vertical pressure applied on soil and initial excess pore pressure, calculation of time-dependent unimproved layer thickness ratio α(t) and computation of total consolidation settlement at time (t). The time-settlement curve, finally, can be drawn for prediction.

3. Laboratory model tests

For investigating the behaviors of improved foundation and verifying the effectiveness of this method, a kind of laboratory model test was performed. The proposed method for calculating consolidation settlement was applied to this test and later the predicted settlements were compared with the measurement.

3.1 Apparatus and test procedure

Figure 13 shows the apparatus used in the model tests under the plane strain condition. This apparatus consists of a box-shaped cell, loading plates and loading device. The box-shaped cell is 250 mm in length, 100 mm in width and 400 mm in height. Perforated acrylic plates were used to model drainage condition at the top and bottom of the model ground. Two types of tests were

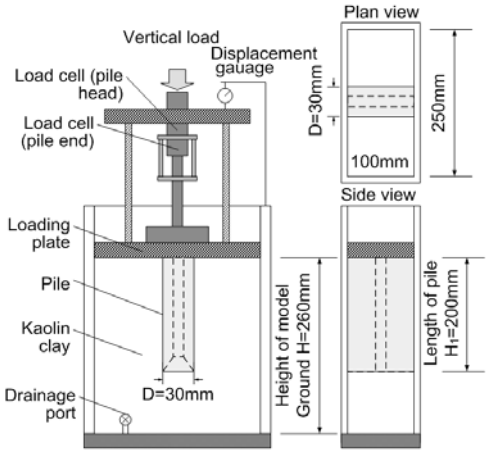

Fig. 13. Loading model test under the plane strain condition.

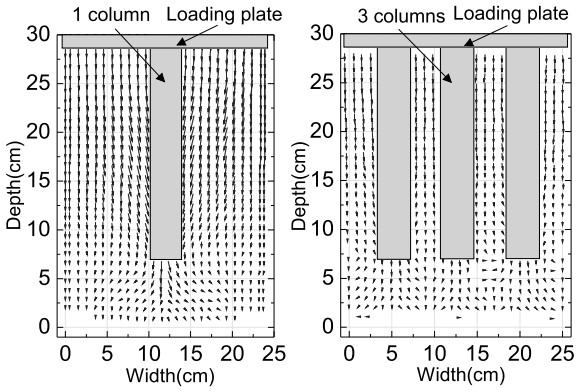

Case1: 1 pile (σ=0→80kPa) Case2: 3 piles (σ=0→80kPa)

Fig. 14. Deformation of the model foundations.

Table 2. Soil properties of Kaolin clay.

Soil particle density ρ_s (g/cm^3)	Liquidity limit w_l (%)	Plastic limit w_p (%)	Plasticity index I_p (%)
2.71	50.6	31.0	19.6
Compression index C_c	Swelling index C_s	Effective cohension c' (kPa)	Effective angle of friction ϕ' (°)
0.365	0.076	5	31.35

Table 3. Consolidation parameters of unimproved ground.

Vertical pressure $\overline{\sigma}$ (kPa)	Coefficient of volume compressibility m_v (m^2/kN)	Consolidation index C_v(cm^2/s)	Coefficient of permeability k_y (m/s)	Compression index C_c
20～40	2.04E-03	6.11E-03	6.12E-09	0.409
40～80	1.58E-03	1.11E-02	8.63E-09	

Table 4. Laboratory model size parameters.

Improved depth H_1 (m)	Unimproved depth H_2 (m)	Ground improvement ratio a_p (%)
0.2	0.07	12, 36
Equivalent radius r (m)	Total ground area A_0 (m^2)	Overburden pressure $\overline{\sigma}$ (kPa)
0.03	0.025	20, 40

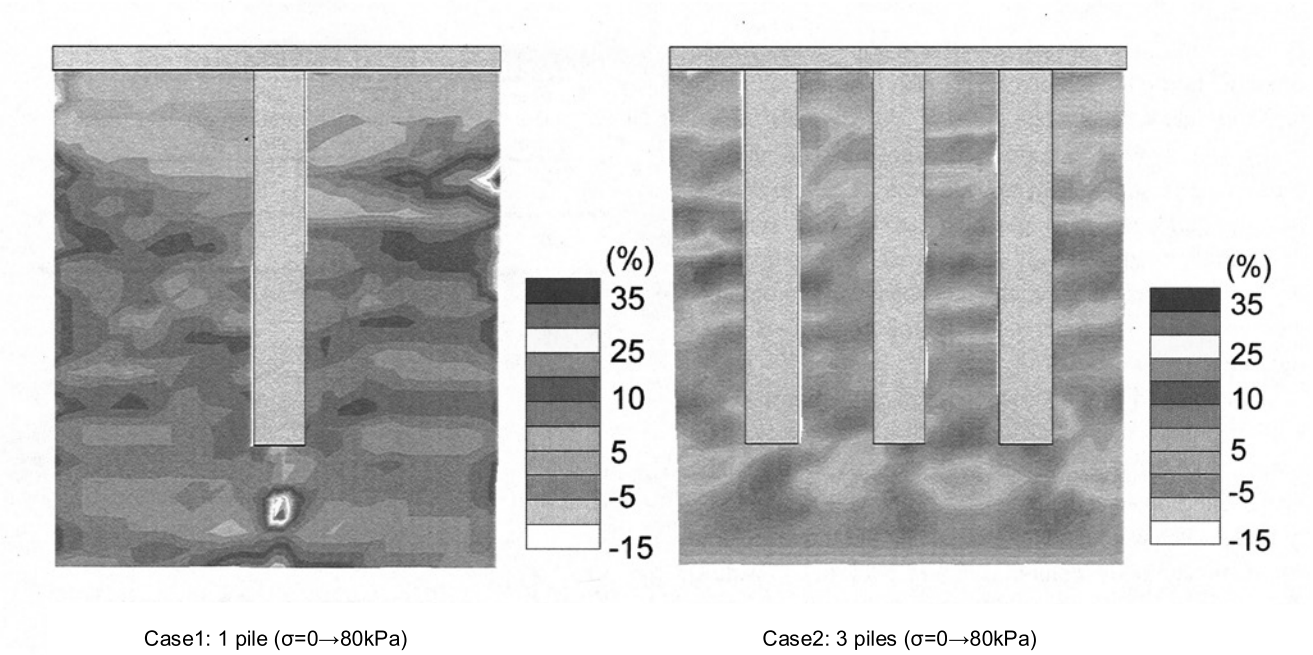

Case1: 1 pile (σ=0→80kPa) Case2: 3 piles (σ=0→80kPa)

Fig. 15. Vertical strain distributions after consolidation.

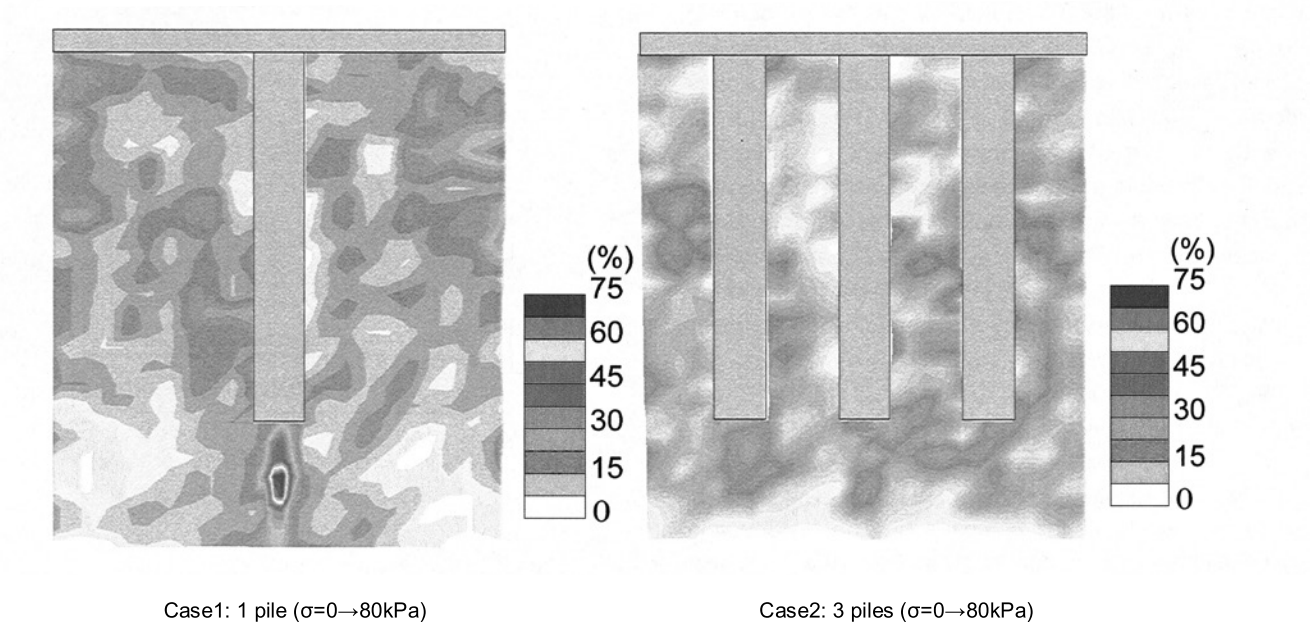

Case1: 1 pile (σ=0→80kPa) Case2: 3 piles (σ=0→80kPa)

Fig. 16. Maximum shear strain after consolidation.

performed. One was unimproved ground for getting the soil consolidation parameters, and the other was improved ground using one and three wall-shape aluminum columns for investing settlement behaviors. This test was performed as following:

1) Model ground preparation. First, the separate acrylic plates were assembled as a square shape box; four rubber membranes were covered on the inside wall using grease for reducing the wall friction. One piece of the membranes was painted grid lines for monitoring the ground deformation. The deformation results can be generated by image analysis of grid lines. Then the model ground was prepared using Kaolin clay, which was remolded in a slurry condition with water content of about 80 %. The properties of the soil are listed in Table 2. At last the slurry was poured into the container layer by layer, until up to a depth of about 350 mm. In order to avoid the uneven soil and the bubble residues in soil, the soil layers were stirred using a steel rod. After the loading system was set up, a pre-consolidation pressure was applied using a bellofram cylinder, from 2.5 kPa to 20 kPa using LIR (Load increment ratio) of one. Each pressure lasted in 24 hours until the end of primary

consolidation. The settlement at the top of the model ground and the pre-consolidation pressure were monitored during this stage.

2) Unimproved ground consolidation. The vertical pressure was sequentially applied from 20 kPa to 80 kPa using LIR of one by using a bellofram cylinder, until the consolidation tests finished. Each pressure also lasted in 24 hours. Consequently, the consolidation parameters were obtained. The main results were listed in Table 3 as following:

3) Improved ground consolidation settlement. At the end of primary consolidation with the pre-consolidation pressure of 20 kPa, the test was stopped. The loading system and one acrylic plate were removed for cutting a groove, which was used for embedding the model column. An aluminum model column with size of 30 mm in wide D, 100 mm in length and 200 mm in height H1, was embedded in the model ground. Then the apparatus were reassembled again, pre-consolidation pressure of 20 kPa was applied firstly for 24 hours to ensure firm contact between the model column and the surrounding soil and to bring the model ground to a normally consolidation state, and then the vertical pressure was increased stepwise from 20 kPa to 80 kPa using LIR of one by using a bellofram cylinder, each pressure still lasted in 24 hours until the tests were finished. During the test, the settlement at the top of the model ground, the vertical load and resistance at the head and end of the column were monitored. Meanwhile, the ground deformation was recorded by a camera directed at rubber membrane's grid lines.

3.2 Test results and discussions

The consolidation settlement will be discussed in detail in section 4 for comparison. The deformation mechanisms of this improved ground are mainly studied in this section. Figure 14 shows the deformation behaviors of the improved ground in two cases, 1 column (Case-1) and 3 columns (Case-2). The vertical pressure increased from 0 kPa to 80 kPa stepwise under the consolidation process. It is observed that vertical deformations occurred over whole area around the column for both cases. Meanwhile, it is also obviously displayed that the consolidation settlements decreased with an increase of the number of columns, manifesting that the deformation in Case-2 is smaller than that in Case-1, and a large deformation of the ground occurred at the bottom of column in Case-1.

Utilizing the image analysis based on experimental results, Fig. 15 presents the vertical strain distributions after consolidation finished in the Case-1 and Case-2, respectively. According to these results, the vertical strain just below the column end increased significantly, and it decreased with the number of columns increasing. On the other hand, the vertical strain just below the loading plate is much smaller than that just below the column end in the both test conditions. This is mainly on account of the effect of surface stabilization, which can reduce the relative movement between the column and surrounding soil. According to the image analysis results, the improved ground can be divided into two layers, confining layer (upper portion with small vertical strain) and compressed layer (lower portion with large vertical strain), a phenomenon similar to that encountered in the problem of estimating the floating type column improved ground settlement (Terzaghi and Peck, 1967). Figure 16 shows the maximum shear strain distributions in Case-1 and Case-2, respectively. The maximum shear strain mainly

Table 5. Forecast error of the model tests.

Number of column	Vertical pressure Δp (kPa)	Ground improvement ratio a_p (%)	Forecast error Δξ (%)
1	20	12	4.72
	40	12	8.83
3	20	36	18.40
	40	36	55.15

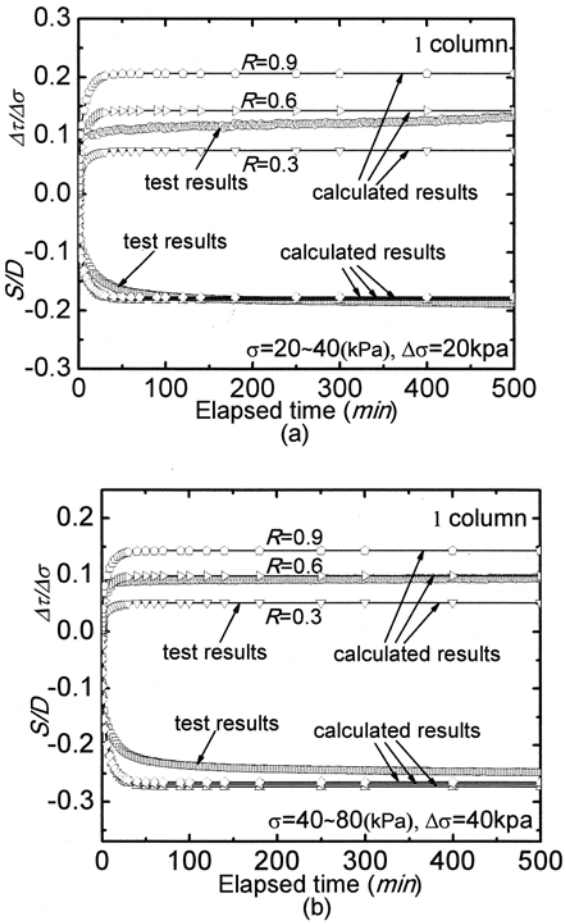

Fig. 17. Comparison between measured and calculated results (1 column).

arose at the end of column in Case-1, and it decreased with the number of columns increased.

4. Validation of the proposed method by model tests

To check the reliability of the proposed method, analyzation is conducted based on two kinds of laboratory model tests as reported in section 3. The parameters used for calculation (1 column and 3 columns) are given in Table 3 (increased vertical pressure are 20 kPa and 40 kPa), the model dimension parameters are listed in Table 4. The relationship between normalized settlements S/D, normalized averaged skin friction $\Delta\tau/\Delta\sigma$ and elapsed time during consolidation process are shown in Figs. 17 and 18. As can be seen, the proposed method yields a good prediction for 20～40 kPa in one column condition. Nevertheless the calculated results are in a larger settlement for the rest conditions. This phenomenon is mainly caused by the influence of boundary conditions of this model. The compression of the unimproved soil layer is primarily decided by the volume compressibility coefficient of soft soil on the basis of Eqs. [22] and [23]. In consequence of the confining acrylic plates, the deformations of unimproved layer (αH_1+H_2) in improved ground are larger than that of same thickness soil layer in unimproved ground under the condition of the same vertical pressure. It resulted in the volume compressibility coefficient of unimproved layer soil in the improved ground (m_v^{u*}) is smaller than that in the unimproved ground (m_v^*). However, m_v^* is used to calculate the compression of the unimproved layer in this paper, hence the calculations are in a larger results. Moreover, the influence is enhanced by the increment of vertical pressure and improvement ratio. On the other hand, the normalized skin friction is calculated using three different interface roughness coefficients, 0.3, 0.6 and 0.9. It is indicated that the interface roughness coefficient between model column and Kaolin clay is around 0.6 from the comparison results, especially from Fig. 17(b) and Fig. 18.

Based on the comparisons, a forecast error ($\Delta\xi$) defined as the ratio between the D-value of prediction and measurement and measured results, is used for describing this phenomenon. The results are listed in Table 5 below:

It can be deduced that the forecast error increased along with the ground improvement ratio as well as the vertical pressure. In spite of this, the tendency of consolidating settlement in calculation results is compatible with that in the experimental results. According to the test process, for instance, the load was

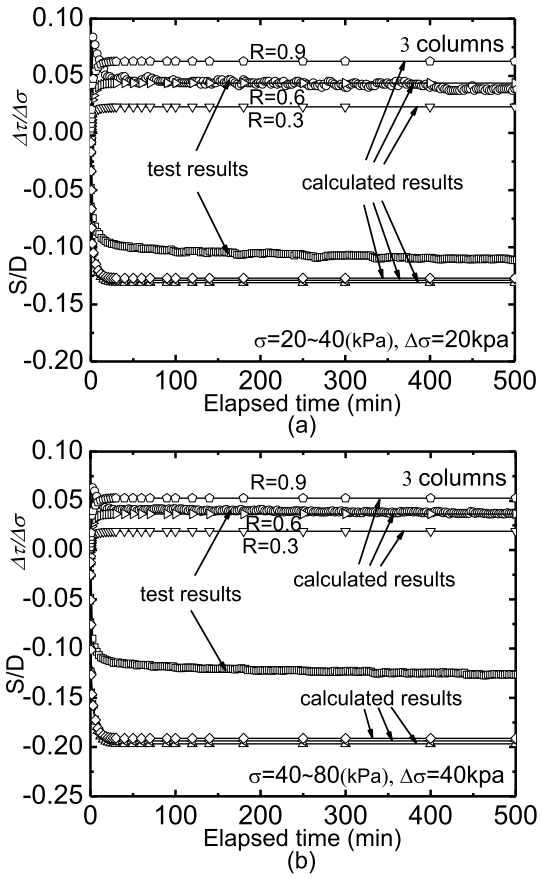

Fig. 18. Comparison between measured and calculated results (3 columns).

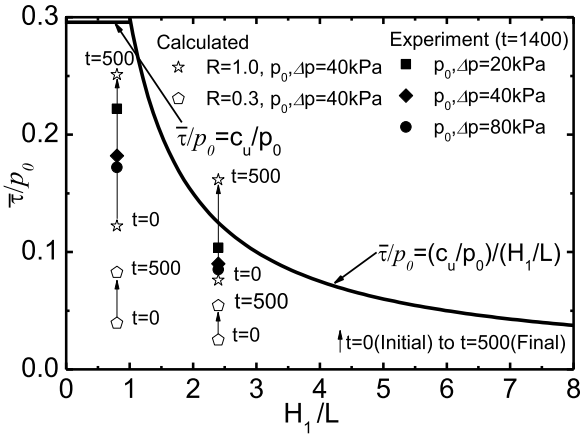

Fig. 19. Comparison between formulation of upward skin friction and experiment results.

applied by stepwise loading, the next loading was applied after the consolidation which caused by the previous loading was completed. As shown in Figs. 17 and 18, the consolidation settlement increased rapidly initially and then converged to the constant value. From these figures, they are shown that the consolidation settlement was mainly completed in a relatively short period when the

pressure was just applied, and the tendency of which also can be observed in calculated results.

Figure 19 shows the comparison between formulation of upward skin friction (Ishikura, et al., 2009) and experiment results, $\bar{\tau}$ is the average upward skin friction, p_0 is the initial vertical pressure at each stage. The value of p_0 is equal to the incremental vertical pressure Δp, and L is the distance between two columns. As shown in this figure, the normalized average upward skin friction increases with consolidating time from calculations. It tends to a constant value when consolidation finished under different ratios between H_1 and L. The experiment results are all within the consolidation process of calculation. They increase with incremental vertical pressure.

5. Conclusions

This article proposed a method for predicting consolidating settlement based on a time-dependent skin friction model. For certifying the effectiveness of this method, a series of laboratory model tests were performed. Meanwhile the image analysis of the settlement behavior during consolidation was conducted. The characteristics of time-depended skin friction, the tendency of consolidation settlement and skin friction of the improved ground, and the effects of improved column number are clarified. The following conclusions can be derived from this study.

(1). Consolidation settlement. It increased initially and then converged to the constant value after applying vertical pressure. And the mainly settlement completed within a relatively short period when the pressure was just applied. The settlement decreased with the increase of column numbers.

(2). Skin friction. Normalized averaged incremental skin friction $\Delta\tau$ initially increased just applying on the vertical pressure, after reaching the peak, it began to decrease with time and later converged to the constant values. Meanwhile, it decreased with the vertical pressure increased under the same ground improvement ratio. For the reason that after static skin friction reaching the ultimate value, the relative slide between column surface and soil or soil interior occurred. Shortly afterwards, sliding friction decreased and later converged to the constant value. The interface roughness coefficient of the model test is around 0.3.

(3). Vertical strain and Maximum shear strain. The vertical strain just below the column end increased significantly during consolidation settlement process. And it decreased with the ground improvement ratio increased. Meanwhile, by the effect of surface stabilization, the relative movement between column and surrounding soil was reduced. The phenomenon is that the vertical strain just below the loading plate is much smaller than that just below the column end. The maximum shear strain mainly generates at the bottom of column, and also decreased with the increasing of the number of columns.

Acknowledgements

The authors wish to express their gratitude to many students, at the graduate school of Kyushu University, for their supports. The second author is grateful to Prof. Y. Nakata of Yamaguchi University for his support with image analysis.

References

Balaam, N.P., Booker, J.R. and Poulos, H.G., 1977. Settlement analysis of soft clays reinforced with granular piles. Proc. 5th Southeast Asian Conference on Soil Engineering, Bangkok, Thailand: 81-92.

Bergado, D.T., Chai, J.C., Alfaro, M.C. and Balasubramaniam, A.S., 1994. Improvement techniques of soft ground in subsiding and lowland environment. Balkema, Rotterdam: 108-121.

Chai, J.C. and Carter, J.P., 2011. Deformation analysis in soft ground improvement. Springer: pp.247

Ishikura, R., Ochiai, H., Omine, K., Yasufuku, N. and Kobayashi, T., 2007. Estimation of the settlement of improved ground with a combined technology of shallow stabilization and floating-type cement treated columns, Proc. JSCE, **63** (4): 1101-1112 (in Japanese).

Ishikura, R., 2008. Estimation of settlement of improved ground using shallow stabilization and floating-type columns, Ph.D. Thesis. Fukuoka: Kyushu Univ., Japan (in Japanese).

Ishikura, R., Ochiai, H., Omine, K., Yasufuku, N., Matsuda, H. and Matsui, H., 2009. Evaluation of the settlement of in-suit improved ground using shallow stabilization and floating-type cement-treated columns, Proc. JSCE, **65** (3): 745-755 (in Japanese).

Ishikura, R., Matsuda H. and Igawa N., 2013. Visualization of settlement behavior for friction pile group during consol-idation. Proc. 18th International Conference on Soil Mechanics and Geotechnical Engineering, Paris: 2759-2762.

Jamsawang, P., Bergado, D.T., Bhandari, A. and Voottipruex, P., 2009. Behabior of stiffened deep cement mixing pile in laboratory, Lowland Technology International, IALT, **11** (1): 20-28.

Kulhawy, F.H., 1984. Limiting tip and side resistance: Fact or fallacy, analysis and design of pile foundations. Proc. Symposium in conjunction with the ASCE National Convention, ASCE, San Francisco, USA: 80-98.

Lee, C.Y., 1993. Settlement of pile group-practical approach. J Geotech Eng Div., ASCE, **119** (9): 1449-61.

Maheshwari, P. and Khatri, S., 2012. Nonlinear analysis of in finite beams on granular bed-stone column-reinforced earth beds under moving loads. Soils and Foundations. **52** (1): 114 -125.

Miller, G.A. and Lutenegger, A.J., 1997. Influence of pile plugging on skin friction in overconsolidated clay. J. Geotech. Engrg. ASCE, **123** (6): 525-533.

Miki, H. and Nozu, M., 2004. Design and numerical analysis of road embankment with low improvement ratio deep mixing method. Geo-trans, ASCE, **126** (12): 147-167.

Ng, K.S., Tan, S.A., 2014a. Design and analyses of floating stone columns. Soils and Foundations, **54** (3): 478-487.

Ng, K.S. and Tan, S.A., 2014b. Simplified homogenization method in stone column designs. Soils and Foundations, **55** (1): 154-165.

Omine, K., and Ochiai, H., 1992. One-dimensional compression propertied of sand-clay mixed soils based on soil structure. JSCE (457-21):127-136 (in Japanese).

Omine, K., Ochiai, H. and Yoshida, H., 1998. Estimation of in-situ strength of cement-treated soil based on a two-phase mixture model. Soils and Foundations, **38** (4): 17-29.

Poulos, H.G., 1994. An approximate numerical analysis of piled-raft interaction. International Journal for Numerical Analytical Methods in Geomechanics, **18** (2): 73-92.

Poungchompu, P., Hayashi, S., Suetsugu, D., Du, Y.J. and Alfaro, M.C., 2010. Performance of raft and pile foundation on soft Ariake clay ground under embankment loading, Lowland Technology International, **12** (1): 41-46.

Pribe, H., 1995. The design of vibro replacement. Ground Engineering, December: 31-46.

Randolph, M.F., 1983. Design of piled raft foundations. Recent Developments in Laboratory and Field Test and Analysis of Geotechnical Problems: 525-537.

Randolph, M.F. and Wroth, C.P., 1979. An analysis of the vertical deformation of pile groups. Géotechnique, **29** (4): 423-39.

Yang, J., Tham, L.G., Lee, P.K.K., Chan, S.T. and Yu, F., 2006. Behaviour of jacked and driven piles in sand soil. Géotechnique, **56** (4): 245-259.

Zhang, Y.P. Chan, D. and Wang, Y., 2012. Consolidation of composite foundation improved by geosynthetic-encased stone columns. Geotextiles and Geomembranes, **32** (6): 10-17.

Symbols and abbreviations

A_0	Cross-sectional area of the improved ground
A_c	Cross-sectional area of the columns
a_p	Ground improvement ratio
c_u	Undrained shear strength of soil
C_v	Consolidation index
D	Model column wide
H	Depth of ground
H_1	Depth of improved layer (column length)
H_2	Depth of unimproved layer
h	Thickness of surface stabilization
K	Lateral earth pressure coefficient
K_0	In situ earth pressure coefficient
L	Loading width on the equivalent foundation
L'	Loading width on the unimproved layer
$\overline{m_v}$	Average coefficient of volume compressibility of composite portion
$\overline{m_{vf}}$	Average coefficient of volume compressibility of the confining portion
m_{vs}	Volume compressibility coefficient of column
m_v^*	Volume compressibility coefficient of soil
m_v^{u*}	Volume compressibility coefficient of unimproved layer soil in the improved ground
$\overline{n}$	Stress distribution ratio
$\overline{n_f}$	Final effective stress distribution ratio
n(t)	Stress distribution ratio during consolidation
p_0	Iinitial vertical pressure at each stage
R	Interface roughness coefficient
S(t)	Total settlement of the improved ground
$S_e(t)$	Compression of the equivalent foundation
$S_u(t)$	Settlement of the unimproved layer
T_v	Time factor for one-dimensional consolidation
u(z,t)	Excess pore pressure
$u_0(z,t)$	Initial excess pore pressure
α	Unimproved layer thickness ratio
α(t)	Unimproved layer thickness ratio during consolidation
α_i	Initial unimproved layer thickness ratio
δ'	Effective friction angle of column-soil interface
σ_v'	Effective overburden pressure
σ'(z,t)	Vertical effective pressure applied on the soft soil during consolidation
σ*(t)	Total vertical pressure applied on the soft soil
σ'(t)	Effective vertical pressure applied on the soil
$\overline{\sigma}$	Vertical pressure applied on the ground
σ_{vs}	Vertical pressure applied on the column

$\overline{\sigma^*}$	Vertical pressure applied on the soil	$\overline{\tau}$	Average skin friction of interface
$\overline{\sigma'(t)}$	Effective vertical pressure applied on the ground during consolidation	$\overline{\tau(t)}$	Average skin friction of interface during consolidation
$\overline{\sigma_b'(t)}$	Average distributive effective vertical pressure on the unimproved layer	ϕ'	Effective friction angle of soil
		$\Delta\xi$	Forecast error
τ	Skin friction of interface	$\Delta\tau$	Increment of skin friction
$\tau(z,t)$	Skin friction of interface during consolidation	$\Delta\sigma$	Increment of vertical pressure